

Costimulation of $\gamma\delta$ TCR and TLR7/8 promotes V δ 2 T-cell antitumor activity by modulating mTOR pathway and APC function

Huashan Wang ¹, Hui Chen,¹ Shujing Liu,¹ Jie Zhang,² Hezhe Lu,³ Rajasekharan Somasundaram,⁴ Robin Choi,⁴ Gao Zhang,^{4,5} Lingling Ou,¹ John Scholler,⁶ Shifu Tian,¹ Liyun Dong,¹ Guo Yeye,¹ Lili Huang,¹ Thomas Connolly,⁴ Ling Li,⁴ Alexander Huang,⁷ Tara C Mitchell,⁷ Yi Fan,⁸ Carl H June,^{1,6,9} Gordon B Mills,¹⁰ Wei Guo,¹¹ Meenhard Herlyn,⁴ Xiaowei Xu ¹

To cite: Wang H, Chen H, Liu S, *et al.* Costimulation of $\gamma\delta$ TCR and TLR7/8 promotes V δ 2 T-cell antitumor activity by modulating mTOR pathway and APC function. *Journal for ImmunoTherapy of Cancer* 2021;**9**:e003339. doi:10.1136/jitc-2021-003339

► Additional supplemental material is published online only. To view, please visit the journal online (<http://dx.doi.org/10.1136/jitc-2021-003339>).

HW and HC contributed equally.
Accepted 04 November 2021



© Author(s) (or their employer(s)) 2021. Re-use permitted under CC BY-NC. No commercial re-use. See rights and permissions. Published by BMJ.

For numbered affiliations see end of article.

Correspondence to

Professor Xiaowei Xu;
xug@penncmedicine.upenn.edu

ABSTRACT

Background Gamma delta ($\gamma\delta$) T cells are attractive effector cells for cancer immunotherapy. V δ 2 T cells expanded by zoledronic acid (ZOL) are the most commonly used $\gamma\delta$ T cells for adoptive cell therapy. However, adoptive transfer of the expanded V δ 2 T cells has limited clinical efficacy.

Methods We developed a costimulation method for expansion of V δ 2 T cells in PBMCs by activating $\gamma\delta$ T-cell receptor ($\gamma\delta$ TCR) and Toll-like receptor (TLR) 7/8 using isopentenyl pyrophosphate (IPP) and resiquimod, respectively, and tested the functional markers and antitumoral effects in vitro two-dimensional two-dimensional and three-dimensional spheroid models and in vivo models. Single-cell sequencing dataset analysis and reverse-phase protein array were employed for mechanistic studies.

Results We find that V δ 2 T cells expanded by IPP plus resiquimod showed significantly increased cytotoxicity to tumor cells with lower programmed cell death protein 1 (PD-1) expression than V δ 2 T cells expanded by IPP or ZOL. Mechanistically, the costimulation enhanced the activation of the phosphatidylinositol 3-kinase (PI3K)–protein kinase B (PKB/Akt)—the mammalian target of rapamycin (mTOR) pathway and the TLR7/8–MyD88 pathway. Resiquimod stimulated V δ 2 T-cell expansion in both antigen presenting cell dependent and independent manners. In addition, resiquimod decreased the number of adherent inhibitory antigen-presenting cells (APCs) and suppressed the inhibitory function of APCs by decreasing PD-L1 and cytotoxic T-lymphocyte-associated protein 4 (CTLA-4) expression in these cells during in vitro V δ 2 T-cell expansion. Finally, we showed that human V δ 2 T cells can be expanded from PBMCs and spleen of humanized NSG mice using IPP plus resiquimod or ZOL, demonstrating that humanized mice are a promising preclinical model for studying human $\gamma\delta$ T-cell development and function.

Conclusions V δ 2 T cells expanded by IPP and resiquimod demonstrate improved anti-tumor function and have the potential to increase the efficacy of $\gamma\delta$ T cell-based therapies.

INTRODUCTION

Personalized adoptive T-cell transfer (ACT) therapies with autologous tumor-infiltrating lymphocytes, T-cell receptor (TCR) T cells, or chimeric antigen receptor T cells have provided major breakthroughs in the treatment of a number of cancers including leukemia, lymphoma, and melanoma.^{1 2} Current ACT research and clinical applications have focused primarily on alpha beta ($\alpha\beta$) T cells, which are human leukocyte antigen (HLA)-restricted in tumor cell recognition.³ During cellular immunotherapy, tumor cells may downregulate or lose HLA class I or β 2 microglobulin, which allows tumor cells to evade detection from $\alpha\beta$ T cells, resulting in immune escape and treatment failure.⁴

Gamma delta ($\gamma\delta$) T cells are an unconventional subset of T cells expressing heterodimeric TCRs composed of γ and δ chains, and they are HLA-unrestricted in tumor cell recognition.⁵ The recognition of cancer antigens, such as phosphoantigens (pAgs), relies on the engagement of $\gamma\delta$ TCR. Thus, tumors may still be targets for $\gamma\delta$ T cells even if they not efficiently recognized by $\alpha\beta$ T cells. High circulating levels of $\gamma\delta$ T cells have been associated with improved 5-year disease-free and overall survival after bone marrow transplantation in patients with acute leukemia.⁶

Toll-like receptors (TLRs) are pattern-recognition receptors that recognize pathogen-associated molecular patterns and/or damage-associated molecular patterns. They are essential receptors in host defense against various pathogens and cancer cells.⁷ Human $\gamma\delta$ T cells express multiple TLRs,

including TLR7 and TLR8,^{8,9} and TLRs interact with $\gamma\delta$ TCR to modulate $\gamma\delta$ T-cell functions.⁹

In humans, two major subsets of $\gamma\delta$ T cells have been identified by the variable (V) gene of $\gamma\delta$ TCR, which are V δ 1 T cells, the predominant population in peripheral tissues and intestine mucosa, and V δ 2 T cells, which represent a majority of $\gamma\delta$ T cells in peripheral blood and coexpress V γ 9 chain of TCR. V γ 9V δ 2 T cells (V δ 2 T cells) are unique in primates, but they only account for less than 5% of total T cells.¹⁰ Most of the $\gamma\delta$ T-cell clinical trials to date have focused on the V δ 2 T-cell subset, given their relative abundance in peripheral blood.¹¹

V δ 2 T cells are commonly expanded using bisphosphonates, such as zoledronic acid (ZOL) and pamidronate, or pAgs, such as isopentenyl pyrophosphate (IPP), a natural intermediate of the mevalonate pathway¹² and the potent microbial compound (E)-4-hydroxy-3-methylbut-2-enyl pyrophosphate (HMBPP). V δ 2 T cells can be expanded over 13 000-fold.¹³ ZOL is the most common compound to expand clinical grade V δ 2 T cells.¹⁴ Limited efficacy has been reported in clinical trials that explored the transfer of ex vivo-expanded autologous or allogeneic V δ 2 T cells. The failures of such strategies likely involve multiple factors, such as $\gamma\delta$ TCR diversity and heterogeneity of the function of V δ 2 cell after expansion. Exhaustion of expanded $\gamma\delta$ T cells is a major issue that has not been addressed.¹⁵

The clinical success of ACT depends on the efficient expansion of T cells in vitro, and perhaps more importantly the quality of the expanded T cells.^{2,16} In the current studies, we discover that costimulation of $\gamma\delta$ TCR and TLR7/8 using IPP and resiquimod effectively expand V δ 2 T cells from peripheral blood mononuclear cells (PBMCs). These expanded V δ 2 T cells show better cytotoxicity and lower expression of PD-1 proteins than V δ 2 T cells expanded by ZOL. Resiquimod enhances the PI3K–Akt–mTOR pathway in V δ 2 T cells and suppresses inhibitory functions of adherent antigen-presenting cells (APCs) in the culture. The new method of in vitro-V δ 2 T cell has the potential to improve the treatment efficacy of $\gamma\delta$ T cell-based therapies.

MATERIALS AND METHODS

Study design

The study presented here was designed to develop a new method to expand V δ 2 T cells from PBMC ex vivo for adoptive T cell therapy (ACT). For in vitro and in vivo biomarker tests and antitumor assays, a minimum of three independent cytotoxicity experiments were performed as detailed further unless otherwise noted. Investigators were not blinded during the in vivo studies. In reverse-phase protein array (RPPA) analysis, each group included five healthy donor PBMC samples, and the data were analyzed by independent and blinded investigators.

Reagents

TLR1/2 agonist Pam3CSK4 (tlrl-pms), TLR2/NOD2 agonist CL429 (tlrl-C429), TLR2/4 agonist lipopolysaccharide (LPS)-EB (LPS from *Escherichia coli* O111:B4, tlrl-eb1ps), TLR4 agonist Monophosphoryl Lipid A (MPLA) Synthetic (tlrl-mpls), TLR5 agonist FLA-ST (flagellin from *Salmonella typhimurium*, tlrl-stfla), TLR7 agonists imiquimod (R837, tlrl-imqs) and gardiquimod (tlrl-gdqs) were purchased from InvivoGen (California, USA). TLR7/8 agonist resiquimod (R848, SML0196), IPP triammonium salt solution (I0503), and ZOL (1724827) were purchased from Sigma-Aldrich (Missouri, USA). Antihuman PD-1 antibody, pembrolizumab (Keytruda, Merck & Co, New Jersey, USA; R014267), was stored at -80°C at 25 mg/mL before use. MyD88 inhibitor ST-2825 was purchased from MedChemExpress (New Jersey, USA). mTOR inhibitors torin1 (S2827; Selleck Chemicals, Texas, USA) and rapamycin (NC9362949, LC Laboratories, MA, USA) were described previously.¹⁷

Primary cells and cell lines

PBMCs and monocytes were obtained from Human Immunology Core at the University of Pennsylvania, which were obtained from healthy donors. For $\gamma\delta$ T-cell expansion, PBMCs were cultured with RPMI1640 media supplemented with 10% FBS (HyClone; GE Healthcare, Utah, USA), 100 U/mL penicillin–streptomycin, 2 mM L-glutamine, 1/1000 2-mercaptoethanol (2-Me) (Gibco; Thermo Fisher Scientific, Massachusetts, USA) (or without 2-Me as indicated) and 200 units/mL of recombinant human interleukin (IL)-2 (PeproTech, New Jersey, USA) in 24-well microplates, new media added and supplemented every other day. $\gamma\delta$ T cells were expanded in 24-well tissue culture treated microplates that were coated with mouse-monoclonal anti-pan-TCR $\gamma\delta$ antibody (1.0 $\mu\text{g}/\text{mL}$ in phosphate-buffered saline (PBS); IMMU510, IM1349, Beckman). For naive $\gamma\delta$ T-cell isolation, PBMCs were purified using a commercial human TCR γ/δ T-cell Isolation Kit (Miltenyi Biotec, Germany). Purified naive $\gamma\delta$ T cells routinely exceeded $>95\%$ concentration by flow cytometry. Human melanoma cell lines A375, A2058, WM9, 903 were obtained from Meenhard Herlyn's laboratory (The Wistar Institute, Philadelphia, Pennsylvania, USA), and they were routinely tested for mycoplasma and DNA fingerprinted.¹⁷ Lung cancer cell line H1975, colon cancer cell line HT-29, and gastric cancer cell line NCI-N87 were purchased from American Type Culture Collection (ATCC). Daudi cells were obtained from Andrei Thomas-Tikhonenko Lab at the University of Pennsylvania and Children's Hospital of Philadelphia, K562 cells were obtained from Michael Milone Lab at the University of Pennsylvania. BRAF inhibitors (BRAFi) and MEK inhibitors (MEKi) combination therapy-resistant (CR) cell lines WM9-CR and A2058-CR were generated as described before.¹⁸

Nude mice and xenograft

All animal procedures were approved by the Institutional Animal Care and Use Committees at the University of Pennsylvania and Wistar Institute. For xenograft, single A375 cell suspensions (2 million in 200 μ L PBS) were injected into the left flank of each nude mouse (Jackson Laboratories) subcutaneously to obtain melanoma xenografts. Six mice per group for human IL-2 (intraperitoneally) only as negative control group, IL-2 (intraperitoneally)+ $\gamma\delta$ T cells (intratumorally) expanded by IPP, and IL-2 (intraperitoneally)+ $\gamma\delta$ T cells (intratumorally) expanded by IPP plus resiquimod. The first treatment was given when palpable tumor could be detected and tumor size reached approximately 50 mm³ and treated four times in 12 days. Tumors were measured with a ruler and volumes were calculated in micrometer (mm) as length \times width \times height/2.

Humanized mice (Hu-mice)

Humanized mice were generated at the Wistar Institute as described.¹⁹ Briefly, the humanized mouse model is developed by reconstituting immunodeficient NSG mice with fetal liver-derived CD34+ human hematopoietic stem cells, grafted intravenously, and autologous fetal thymus chunks, grafted under the renal capsule, to promote rapid human T-cell differentiation.

Flow cytometry

PBMCs and $\gamma\delta$ T-cell phenotypes were analyzed by flow cytometry. Briefly, single-cell suspensions were surface-stained for 30 min at 4°C in the dark, and intercellular staining was performed for 60 min after fixation and permeabilization using a True-Nuclear Transcription Factor Buffer Set (BioLegend, California, USA). Carboxy-fluorescein succinimidyl ester (CFSE) Cell Proliferation Kit for flow cytometry was purchased from Invitrogen (Thermo Fisher). Fluorescein-conjugated antibodies are listed in online supplemental table S4. Data were acquired on LSRA/B or Fortessa B flow cytometers (BD Biosciences, New Jersey, USA) at Flow Cytometry and Cell Sorting Resource Laboratory at the University of Pennsylvania and analyzed with FlowJo software (Tree Star, Ashland, Oregon, USA).

ELISA

Interferon gamma (IFN- γ), IL-17A, and tumour necrosis factor alpha (TNF- α) levels of supernatant were determined by using commercial human ELISA kits from BioLegend (430104, 433914, and 430204, respectively). PBMCs were cultured in a 24-well microplate; supernatants were harvested and centrifuged at 5000 rpm for 5 min to remove lymphocytes without further purification. Samples were aliquoted and stored at -80°C until use and detected.

Cytotoxicity

Cytotoxicity of $\gamma\delta$ T cells against melanoma cells was measured by lactate dehydrogenase (LDH) release using the CytoTox 96 Non-Radioactive Cytotoxicity Assay kit

(G1780; Promega, Wisconsin, USA) as described.²⁰ Briefly, melanoma cells were seeded at 4×10^4 cells/well in 50 μ L standard growth medium in 96-well plates, while $\gamma\delta$ T cells were seeded at effector:target (E:T) ratio (E:T=5:1) in the same volume of PBMC culture media at the same time. After the indicated time, plates were spin down briefly and 50 μ L supernatants were then harvested for further analysis. Absorbance at 490 nm was read using a BioTek Synergy HT reader (BioTek Instruments, Vermont, USA) after LDH activity detection, the percentage of cytotoxicity was calculated as (experimental-effector spontaneous-target spontaneous)/(target maximum-target spontaneous) \times 100.

Melanoma spheroid

Multicellular melanoma spheroids were cultured as described.²¹ Briefly, the 96-well plate was precoated with 50 μ L 1.5% agarose before seeding CFSE (Thermo Fisher) labeled A2058 melanoma cells at 2×10^4 cells/well and allowed to form spheroids over 48 hours. After coculturing with $\gamma\delta$ T cells, an annexin V/propidium iodide (PI) or PI (Biolegend) staining was performed for further analysis by flow cytometry or confocal microscope, respectively. The supernatant was harvested for cytotoxicity by LDH releasing assay (Promega) as described earlier.

Single-cell RNA sequencing (scRNA-seq) dataset scRNA-seq data of sorted $\gamma\delta$ (V δ 2) T cells from three healthy human donor PBMCs were published by Pizzolato *et al.*²² and obtained from NCBI GEO data set repository (GSE128223). Three preprocessed mRNA datasets of GSM3667468 (763 cells), GSM3667470 (1277 cells), and GSM3667472 (1720 cells) were downloaded and analyzed with pipelines provided by Seurat Package.²³

Identification of markers of $\gamma\delta$ T-cell fates and cluster analysis of signaling pathways

To characterize the stage of maturation of $\gamma\delta$ T cells, seven upregulated genes (NKG7, GZMA, IFNG, GZMB, FCGR3A, CST7, and KLRF1) and downregulated genes (CCR7, LEF1, LTB, SELL, and IL7R) during $\gamma\delta$ T-cell activation and differentiation were employed as makers for cluster analysis. All three donor $\gamma\delta$ T cells were combined for the uniform manifold approximation and projection (UMAP) representation. Cut-off setting was performed on each gene within each cell as 25% of all 12 genes to identify naive cells and terminally differentiated effector memory T cells. Kyoto Encyclopedia of Genes and Genomes (KEGG) pathway and Genontology (GO) analysis of significantly different expression genes of naive $\gamma\delta$ T cells and terminally differentiated effector memory T cells were performed using DAVID bioinformatics resources.²⁴ ²⁵ Phosphoproteins in Functional_Categories analysis were specifically analyzed for signaling pathways. The single-sample gene set enrichment analysis (ssGSEA) of single cell selected were performed as described.²⁶

RPPA assay

RPPA assay was performed as described previously.¹⁷ PBMCs from five healthy donors were cultured with IPP (5 µg/mL) or IPP (5 µg/mL) plus resiquimod (10 µg/mL) for 3 or 4 days, then harvested and lysed for RPPA analysis. The array was probed with 297 antibodies and profiled by the RPPA platform at the MD Anderson Functional Proteomics Core facility by a standard operating practice as described previously.²⁷ KEGG pathway and GO analysis were performed as described earlier.^{24,25} Heat maps were generated using Multiple Experiment Viewer (WebMeV) software as described.²⁵

Statistical analysis

Statistical analysis was performed with GraphPad V.6.0 (Prism software package version) and Microsoft Excel 2016 software. Data are presented as mean±SEM, and significant differences were examined with paired Student's t-test. A p value of <0.05 was considered statistically significant.

RESULTS

TLR agonists enhance Vδ2 T-cell expansion in vitro

To identify TLR agonists that are costimulators for Vδ2 T-cell expansion in vitro, we screened several TLR agonists that were reported as potential adjuvants,⁷ including Pam3CSK4 (TLR1/2, 0.3 µg/mL), CL429 (TLR1&NOD2, 10 µg/mL), LPS-EB (TLR4, 10 µg/mL), MPLA (TLR4, 10 µg/mL), FLA-ST (TLR3, 10 µg/mL) and resiquimod (TLR7/8, 10 µg/mL) with IPP (5 µg/mL) (figure 1A and online supplemental material S1A). Although Vδ2 T cells in PBMCs from different donors showed different degrees of responses to IPP, nearly all TLR agonists demonstrated costimulatory effect (figure 1A). Since we are interested in discovering small molecule stimulators that may be used to expand clinical grade γδ T cells, we focused our research on the TLR7/8 agonists, which are clinically available or have been tested in clinical trials. We compared the costimulatory effect of three imidazoquinoline TLR7/8 agonists, imiquimod, gardiquimod and resiquimod on Vδ2 T-cell expansion from PBMCs. The result showed that all three TLR7/8 agonists promoted Vδ2 T-cell expansion (figure 1B,C), but resiquimod showed the best efficacy with the least cytotoxicity. IPP plus resiquimod induced proliferation of Vδ2 T cells specifically, but not other cell populations, including CD56+ NK cells, in PBMCs (online supplemental figure S1B,C). 2-Mercaptoethanol, an antioxidant used in the culture medium, did not affect Vδ2 T-cell expansion (online supplemental figure S1D). Resiquimod also enhanced IPP-induced proliferation of purified γδ T cells from PBMC. Costimulation of purified γδ T cells with IPP plus resiquimod induced more cell proliferation (CFSE dye dilution) and bigger colonies than IPP alone (figure 1D,E). TLR agonists alone showed only a modest effect on purified γδ T-cell expansion (online supplemental figure S2A). The naïve γδ T cells express a similar

level of TLR7 as monocytes but a lower level of TLR8 than monocytes (online supplemental figure S2B).

The costimulatory effect of resiquimod was not only seen in IPP-induced Vδ2 cell expansion but also in pan-anti-γδTCR antibody-mediated Vδ2 T-cell expansion (online supplemental figure S3A-E). In addition, we found that the costimulatory effect of resiquimod was dependent on the simultaneous activation of γδTCR and TLR7/8 during the early stage of Vδ2 T-cell expansion. The addition of resiquimod to IPP containing Vδ2 T culture at day 5 did not increase the yield of Vδ2 T cells (online supplemental figure S4). We recently discovered that there is large interindividual heterogeneity of Vδ2 cell expansion capacity that is independent of expansion methods.²¹ Vδ2 T-cell expansion capacity correlated well with basal Vδ2 cell concentration in the PBMCs.²¹ Since different donors were used in the experiments, this interindividual heterogeneity contributes to the variability of Vδ2 T-cell expansion efficiency seen in the data.

TLR7/8 activation regulates Vδ2 T-cell functional marker expression and cytokine release

To gain insight into TLR7/8 activation-induced functional changes in Vδ2 T cells, we determined the expression of functional markers and secretion of cytokines after expansion. Compared with expansion by IPP only, Vδ2 T cells expanded by IPP plus resiquimod showed more activation potential by expressing lower level of PD-1 and higher level of CD86 after 8 days of culture, while there was no significant change in CTLA-4 level (figure 2A–C). Meanwhile, IFN-γ, TNF-α and IL-17A protein levels in the medium (figure 2) and expression levels of cytotoxicity markers, granzyme B and CD107a (figure 2G–H) were significantly elevated in Vδ2 T cells expanded by IPP plus resiquimod than by IPP alone. No significant change of Fas-ligand and NKG2D was detected (figure 2I,J). These results support that resiquimod increases antitumor function and decreases the potential exhaustion of Vδ2 T cells in the culture.

TLR7/8 activation enhances cytotoxicity of Vδ2 T cells both in vitro and in vivo

γδ T cells were expanded by IPP or pan-anti-γδTCR antibody with or without resiquimod for approximately 13 days. Expanded γδ T cells were incubated with melanoma cells (903 cells) at different E:T ratios of 10:1, 5:1, 2.5:1, and 1.25:1. E:T ratio=5:1 showed the best tumor killing and less spontaneous LDH releasing (online supplemental figure S5). E:T ratio=5:1 was used for other cytotoxicity assays in vitro. Different types of tumor cells, such as melanoma, lung cancer, gastric cancer, and colon cancer cells were tested. Resiquimod significantly enhanced the cytotoxic effect of γδ T cells expanded using IPP or pan-anti-γδTCR antibody to two melanoma cell lines that were resistant to BRAF inhibitor and MEK inhibitor combination therapy (A2058CR and WM9CR)¹⁸ (figure 3A), and to gastric, colon and lung cancer cells (online supplemental figure S6). Three-dimensional

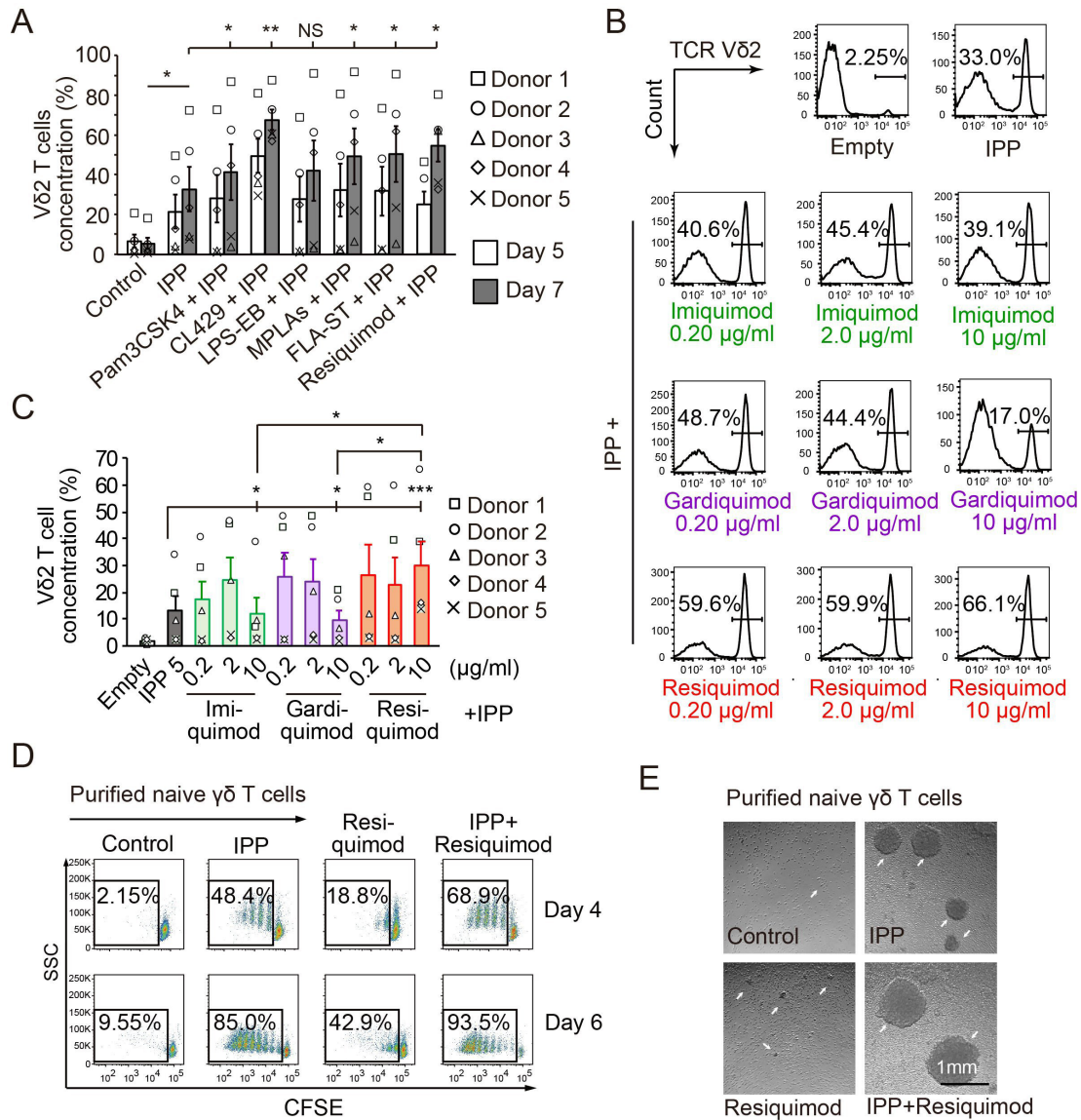


Figure 1 $\gamma\delta$ TCR and TLR costimulation promotes V δ 2 T-cell expansion. (A) Concentrations of human V δ 2 T cells in cultured PBMCs at day 5 or 7. Two million PBMCs were added in each well. IPP (5 μ g/mL) and different TLR agonists were added in each well. Concentrations of V δ 2 T cells were measured by FACS (n=5). (B,C) Concentrations of human V δ 2 T cells in cultured PBMCs at day 7 after costimulation with IPP and different TLR7/8 agonists. Different concentrations of TLR7/8 agonists were used, and representative flow charts are shown in (B) and statistical analysis in (C). n=5. Data are presented as mean \pm SEM. *P<0.05, **P<0.01, ***P<0.001. (D) Purified naive $\gamma\delta$ T cells from PBMCs were cultured with indicated stimulation for 4 and 6 days. Purified naive $\gamma\delta$ T cells (100 K) were labeled with CFSE and added to each well. Rapid dividing cells (daughter cells) are determined to be cells showing a decrease in MFI compared with the initial CFSE staining level. Flow was gated on fast dividing cells (CFSE diluted daughter cells). (E) Brightfield photos of cultured purified naive $\gamma\delta$ T cells at day 4. Purified naive $\gamma\delta$ T cells (100 K) were added to each well and then cultured with indicated compounds. Scale bar indicates 1 mm. FLA-ST, flagellin from *Salmonella typhimurium*; IPP, isopentyl pyrophosphate; MFI, mean fluorescence intensity; NS, no significant difference; PBMC, peripheral blood mononuclear cell; TCR, T-cell receptor; TLR, toll-like receptor; FSC, forward scatter; SSC, side scatter.

melanoma spheroids (A2058) were cultured with V δ 2 T cells expanded by IPP or IPP plus resiquimod and stained with CFSE and propidium iodide (PI). V δ 2 T cells expanded by IPP and resiquimod induced significantly more PI stained dead tumor cells (figure 3B, red), more early (Annexin V+PI-) and late (Annexin V+PI+) apoptotic cells by FACS (figure 3C,D), and significantly more cell death by LDH cytotoxicity assay (figure 3E). We then tested the antitumor effect of the $\gamma\delta$ T cells in a nude

mouse xenograft model (figure 3F). A375 melanoma cells were injected into the flank of nude mice. When the tumor became palpable (50–100 mm³), expanded V δ 2 T cells were injected intratumorally. IL-2 was given intraperitoneally to sustain V δ 2 cells in vivo. V δ 2 T cells expanded by either IPP or IPP plus resiquimod significantly reduced tumor volume compared with the control group that was treated with IL-2 alone (figure 3G). These

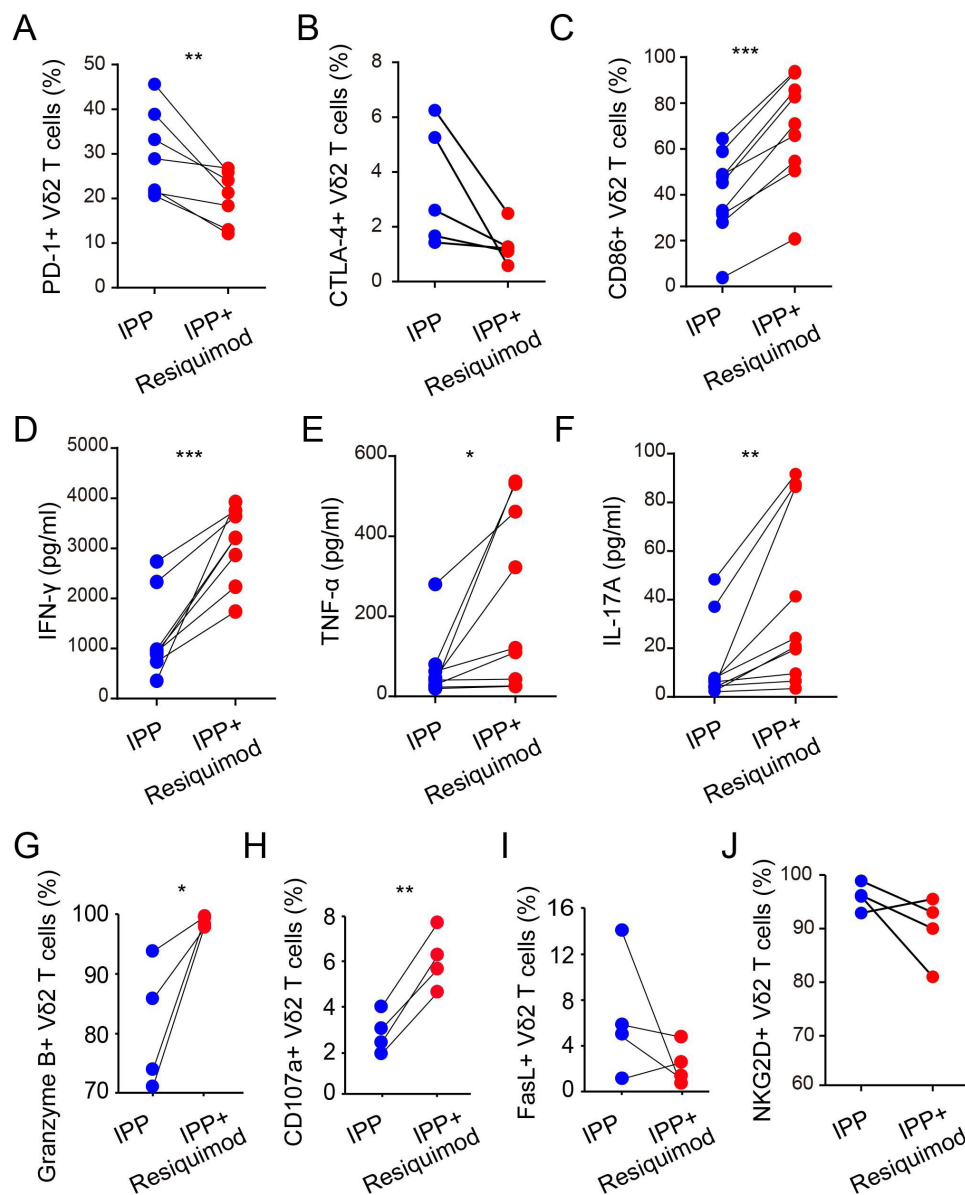


Figure 2 TLR7/8 activation regulates functions of expanded V δ 2 T cells. (A–C) PD-1 (A), CTLA-4 (B), and CD86 (C) expressions in V δ 2 T cells. PBMCs from different donors were used in the experiments and each paired dot represented one donor. Two million PBMCs were added to each well and cultured with IPP or IPP plus resiquimod for 8 days. Protein expression on V δ 2 T cells was measured by FACS. (D–F) IFN- γ (D), TNF- α (E), and IL-17A (F) concentrations in the medium. PBMCs were cultured with IPP or IPP plus resiquimod for 8 days. Cytokine levels in the culture supernatant were measured by ELISA. (G–I) Cytotoxicity-associated marker expression on V δ 2 T cells. PBMCs were cultured with IPP or IPP plus resiquimod for 8 days. Granzyme B (G), CD107a (H), FasL (I), and NKG2D (J) expressions in V δ 2 T cells were measured by FACS. * $P < 0.05$, ** $P < 0.01$, *** $P < 0.001$. FasL, Fas-ligand; IFN- γ , interferon gamma; IL, interleukin; IPP, isopentenyl pyrophosphate; PBMC, peripheral blood mononuclear cell; TLR, toll-like receptor; TNF- α , tumour necrosis factor alpha.

results support that costimulation of $\gamma\delta$ TCR and TLR7/8 promotes $\gamma\delta$ T-cell cytotoxic functions and enhance tumor control.

TLR7/8 activation enhances the PI3K–Akt–mTOR signaling pathway in V δ 2 T cells

To explore the underlying mechanisms of V δ 2 T-cell proliferative capacity and costimulation of $\gamma\delta$ TCR and TLR7/8 in V δ 2 T cells, we analyzed published V δ 2 T-cell scRNA-seq data from three healthy donors.²² The maturation status of V δ 2 T cells was assessed using 12 genes that

were selected based on genes associated with V δ 2 T-cell activation and maturation (J Jacques Fournié, unpublished dataset form in 2020). These genes included genes that were upregulated in V δ 2 T-cell activation and maturation, including NKG7, GZMA, IFNG, GZMB, FCGR3A, CST7, and KLRF1, and downregulated genes including, CCR7, LEF1, LTB, SELL, and IL7R (online supplemental figure S7A, Table S1). Clustering by UMAP identified three clusters of V δ 2 T cells that represented naive, terminally differentiated effector memory and other

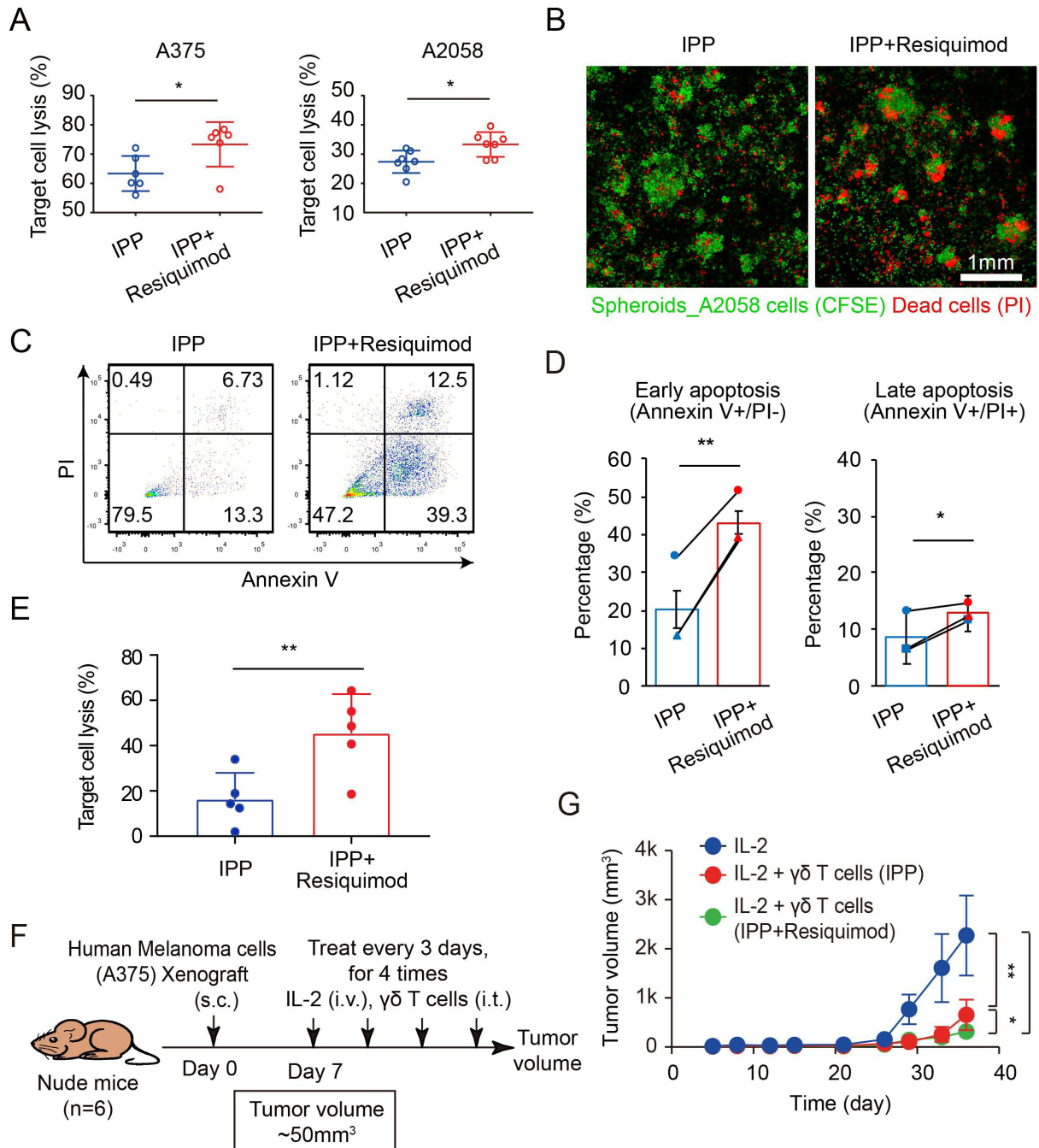


Figure 3 TLR7/8 activation promotes cytotoxicity of V δ 2 T cells. (A) Cytotoxicity of expanded V δ 2 T cells to melanoma cells in two-dimensional culture. V δ 2 T cells were expanded from PBMCs using IPP or IPP plus resiquimod for approximately 13 days. 2×10^4 A375 and A2058 melanoma cells were used in each well. E:T ratio was 5:1 in the coculture. LDH release assay was performed after coculturing V δ 2 T cells and melanoma cells for 16 hours. (B) Cytotoxicity of expanded V δ 2 T cells to melanoma cells in three-dimensional culture. A2058 melanoma spheroids were coculturing with V δ 2 T cells expanded using IPP or IPP plus resiquimod for 24 hours. Green denotes CFSE-stained viable tumor cells, while red denotes PI-stained dead cells. Representative confocal immunofluorescence images show cell death after treatment. Scale bar 1 mm. (C,D) Apoptosis and cell death in A2058 melanoma spheroids after coculturing with V δ 2 T cells. Representative flowcharts after coculturing for 24 hours (C) and statistical analysis of early and late apoptosis cells (D). Each paired dot represents one healthy donor. Data are shown as mean \pm SEM. (E) LDH release assay showing cell death in A2058 melanoma spheroids after coculturing with V δ 2 T cells. Data are shown as mean \pm SEM. (F) Treatment schema of A375 melanoma xenograft model treated with V δ 2 T cells. 5×10^6 melanoma cells were injected into the flanks of nude mice (n=6). V δ 2 T cells from three different donors were expanded from PBMCs using IPP or IPP plus resiquimod for 13 days. The last donor was a good expander, and V δ 2 T cells from the last donor were used to treat all the mice twice. Expanded V δ 2 T cells from a donor were injected into all the mice to avoid donor-related bias. (G) Melanoma tumor volume after treatment. Tumor volume was measured at least two times per week. All data are shown as mean \pm SEM. *P<0.05, **P<0.01, ***P<0.001. E:T, effector:target; IPP, isopentnyl pyrophosphate; LDH, lactate dehydrogenase; PBMC, peripheral blood mononuclear cell; PI, propidium iodide; TLR, toll-like receptor.

memory cells, respectively, demonstrating the distinct maturation and fate stages of V δ 2 T cells (figure 4A–C). Signaling pathway analysis (figure 4 and online supplemental figure S7B) and ssGSEA (figure 4F–H and online supplemental figure S7C) of selected naive cell cluster and terminally differentiated effector memory cell cluster were performed and, in particular, indicated that the PI3K–Akt pathway is one of the most relevant pathways in the process.

The RPPA data also showed that multiple pathways were activated, particularly, the PI3K–Akt–mTOR pathway (figure 4I,J and online supplemental figure S8, and tables S2,3). To confirm the findings, we used two mTOR inhibitors, rapamycin and torin1, to inhibit the mTOR signaling in V δ 2 T cells. We found that the expansion of V δ 2 T cells induced by IPP was significantly reduced, and the inhibition was more prominent in V δ 2 T cells expanded by IPP plus resiquimod (figure 4K,L). In addition, we inhibited the TLR7/8–MyD88 pathway by a MyD88 dimerization inhibitor, ST2825, and found that inhibition of TLR7/8–MyD88 pathway eliminated the costimulatory function of resiquimod (figure 4M,N). These results support the idea that resiquimod promotes V δ 2 T-cell proliferation through the TLR7/8–MyD88 and PI3K–Akt–mTOR signaling pathways.

Advantages of V δ 2 T-cell expansion by IPP plus resiquimod over bisphosphonates

ZOL is the most commonly used agent to expand V δ 2 T cells from PBMCs as it is more efficient than IPP to induce V δ 2 T-cell expansion. We compared the efficiency of V δ 2 T-cell expansion using ZOL versus IPP plus resiquimod. Our data showed that the expansion rate of $\gamma\delta$ T cells using IPP plus resiquimod was comparable with ZOL (figure 5A–C and online supplemental figure S9A). However, V δ 2 T cells expanded by IPP plus resiquimod expressed higher levels of granzyme B and IFN- γ and a lower level of PD-1 compared with ZOL-induced expansion (figure 5D). Furthermore, IPP plus resiquimod expanded V δ 2 T cells showed more cytotoxicity against A375 melanoma cells and Daudi and K562 lymphoma cells than V δ 2 T cells expanded by ZOL (figure 5E and online supplemental figure S9B). Interestingly, expansion of PBMCs with ZOL and resiquimod did not increase V δ 2 T-cell expansion but rather decreased the yield of V δ 2 T cells, particularly in higher concentrations (figure 5F,G, and online supplemental figure S9C), which is similar to the result shown by Serrano *et al* recently.²⁸

APCs are essential for V δ 2 T cell expansion induced by ZOL. APCs release IPP to the surrounding microenvironment and present pAgs to $\gamma\delta$ TCR by BTN3A1 and BTN2A1.²⁹ Using purified naive $\gamma\delta$ T cells from PBMC and CFSE staining, we found that TLR7/8 activation promoted IPP, but not ZOL, and induced V δ 2 T-cell proliferation (figure 5H,I, and online supplemental figure S9D). However, when PBMCs (CFSE– population in online supplemental figure S9D) which contain monocyte-derived dendritic cells were added in the

culture system, ZOL regained the capability of inducing V δ 2 T cell (CFSE+) proliferation (figure 5H,I, and online supplemental figure S9D; ZOL +PBMCs). These results demonstrate that although the expansion efficiency of IPP plus resiquimod is equivalent to ZOL, these two expansion methods are mechanistically different. IPP plus resiquimod induced V δ 2 T-cell expansion in a manner that is independent of APCs.

TLR7/8 agonist suppresses inhibitory function of adherent APCs

APCs are derived from CD14+ monocytes in the PBMCs during in vitro culture, which are adherent and highly express CD80 that binds to CD28 and CTLA-4.³⁰ Adherent APCs from PBMCs cultured with IPP or IPP plus resiquimod were distinctively different. Abundant adherent cells were present in the PBMCs cultured with IPP, but few with IPP plus resiquimod (figure 6A). Further analysis demonstrated that the adherent cells were CD14-CD80+, and they highly expressed PD-L1 and CTLA-4 (figure 6B). CD80+ cells were rare in fresh isolated PBMCs, but all CD80+ cells were highly expressed CD14, PD-L1, and CTLA-4 (online supplemental figure S10A). Resiquimod induced apoptosis and cell death in some monocytes (online supplemental figure S10B–C). These results suggest that CD14+ monocytes in PBMCs give rise to the adherent CD80+ APCs that express high levels of PD-L1 and CTLA-4.

To further decipher the function of adherent APCs during $\gamma\delta$ T-cell expansion, we isolated the adherent APCs after culturing PBMCs with IPP for 3 days. These adherent cells were then added to PBMCs from the same donor that has been stimulated with IPP, IPP plus resiquimod, or ZOL for 3 days. Cells were harvested for V δ 2 T-cell FACS analysis 3 additional days later. In a separate group, adherent cells and resiquimod were added to PBMCs that had been stimulated with IPP for 3 days to test whether the timing of TLR7/8 activation affected V δ 2 T-cell proliferation. The results showed that adherent APCs significantly inhibited the enrichment of V δ 2 T cells induced by IPP plus resiquimod and ZOL (figure 6C,D). The effect of TLR7/8 activation occurred early during V δ 2 T-cell expansion as the addition of resiquimod at day 3 did not affect V δ 2 T-cell expansion (figure 6C,D). To further evaluate the inhibitory role of APCs, we analyzed checkpoint protein expression on CD80+CD86+ APCs in the cultured PBMCs (both adherent and non-adherent cells) after incubation with IPP, resiquimod, IPP plus resiquimod or ZOL, respectively. We found that the presence of resiquimod, with or without IPP, inhibited the expression of PD-L1 and CTLA-4 on CD80+CD86+ APCs (figure 6E–G). However, anti-PD1 antibodies failed to reverse the inhibitory effect of APCs in V δ 2 cell expansion induced by IPP and functional marker expression (online supplemental figure S11). These results support that activation of TLR7/8 suppresses formation of adherent APCs and their inhibitory functions.

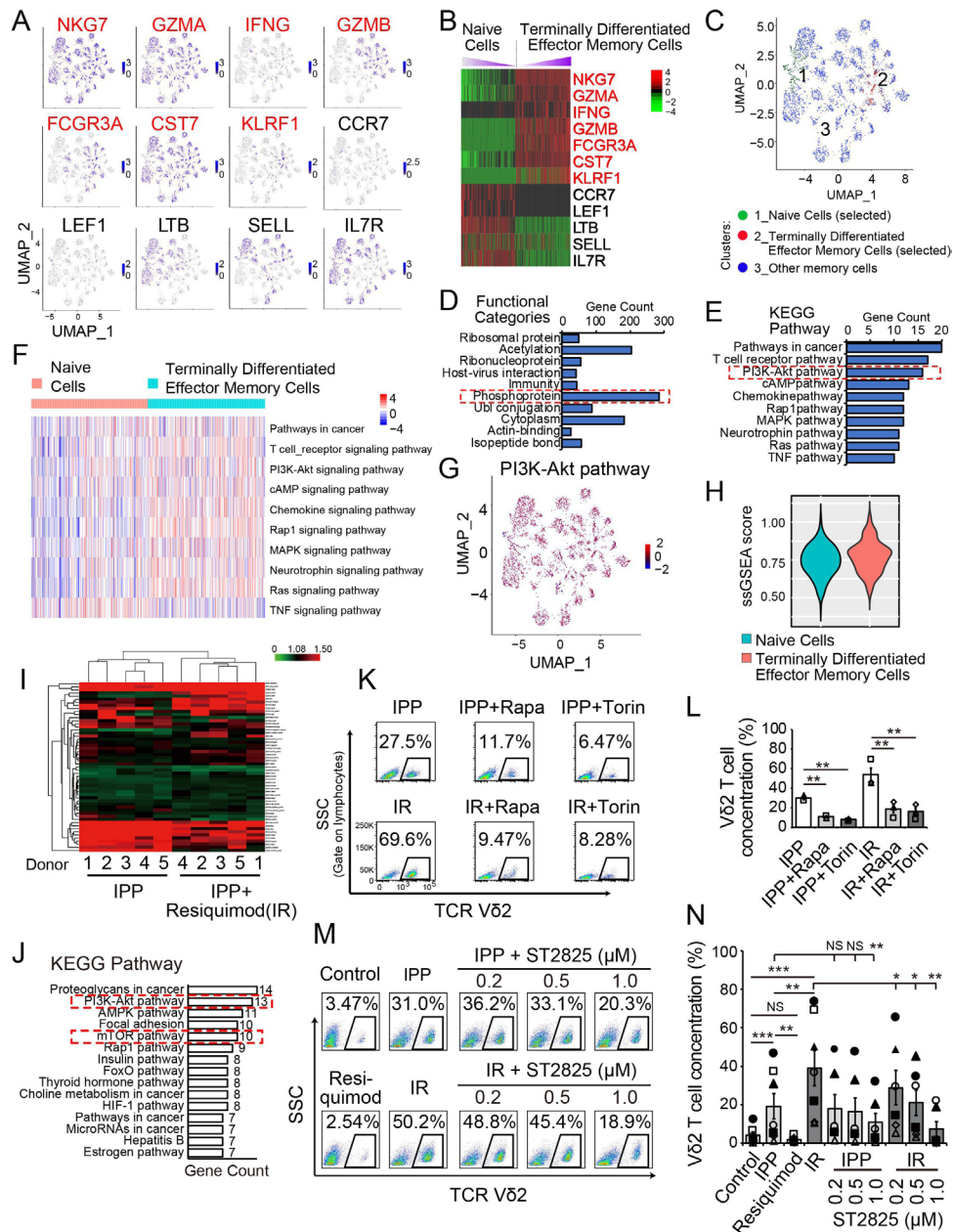


Figure 4 TLR7/8 agonist activates MyD88-dependent and PI3K–Akt–mTOR signaling pathways in V δ 2 T cells. (A) Two-dimensional UMAP panel showing the cluster analysis of V δ 2 T cells with relative expression of seven upregulated genes (red) and five downregulated genes (black) identified as unique to $\gamma\delta$ T-cell activation and differentiation. scRNA-seq data from three healthy donors were analyzed. (B) Heat map showing marker gene expression hits in naive V δ 2 T cells and terminally differentiated effector memory V δ 2 T cells. (C) UMAP sets showing clusters of selected naive V δ 2 T cells and terminally differentiated effector memory V δ 2 T cells for further analysis. (D) Functional categories of significantly different hits between selected naive V δ 2 T cells and terminally differentiated effector memory V δ 2 T cells. (E) KEGG pathway analysis of phosphoprotein of significantly different hits in (D). (F) Heat map showing the ssGSEA of single cell selected. (G) UMAP showing ssGSEA score of PI3K–Akt signaling pathway-related genes. (H) Violin plots showing the ssGSEA score of PI3K–Akt signaling pathway related genes. (I) Heat map of cluster analysis of significantly different protein hits of RPPA assay analysis. (J) KEGG pathway analysis of significantly different protein hits of RPPA assay analysis. (K) Inhibition of V δ 2 T-cell expansion from PBMCs by mTOR inhibitors. PBMC was incubated with IPP or IPP plus resiquimod as well as mTOR inhibitors, Rapa or Torin. Representative flow cytometry results showing the concentrations of V δ 2 T cells. (L) Statistical analysis of K, data shown as mean \pm SEM. (M) Inhibition of V δ 2 T-cell expansion from PBMCs by a MyD88 inhibitor ST2825. PBMCs were incubated with IPP or IPP plus resiquimod as well as ST2825 with indicated concentrations. Representative flow cytometry results showing the concentration of V δ 2 T cells. (N) Statistical analysis of M; data are shown as mean \pm SEM. * P <0.05, ** P <0.01, *** P <0.001. IFN, interferon; IPP, isopentenyl pyrophosphate; KEGG, Kyoto Encyclopedia of Genes and Genomes; NS, no significant difference; PBMC, peripheral blood mononuclear cell; Rapa, rapamycin; RPPA, reverse-phase protein array; scRNA-seq, single-cell RNA sequencing; ssGSEA, single-sample gene set enrichment analysis; TCR, T-cell receptor; TLR, toll-like receptor; TNF, tumour necrosis factor; Torin, torin1; UMAP, uniform manifold approximation and projection.

Figure 5 A

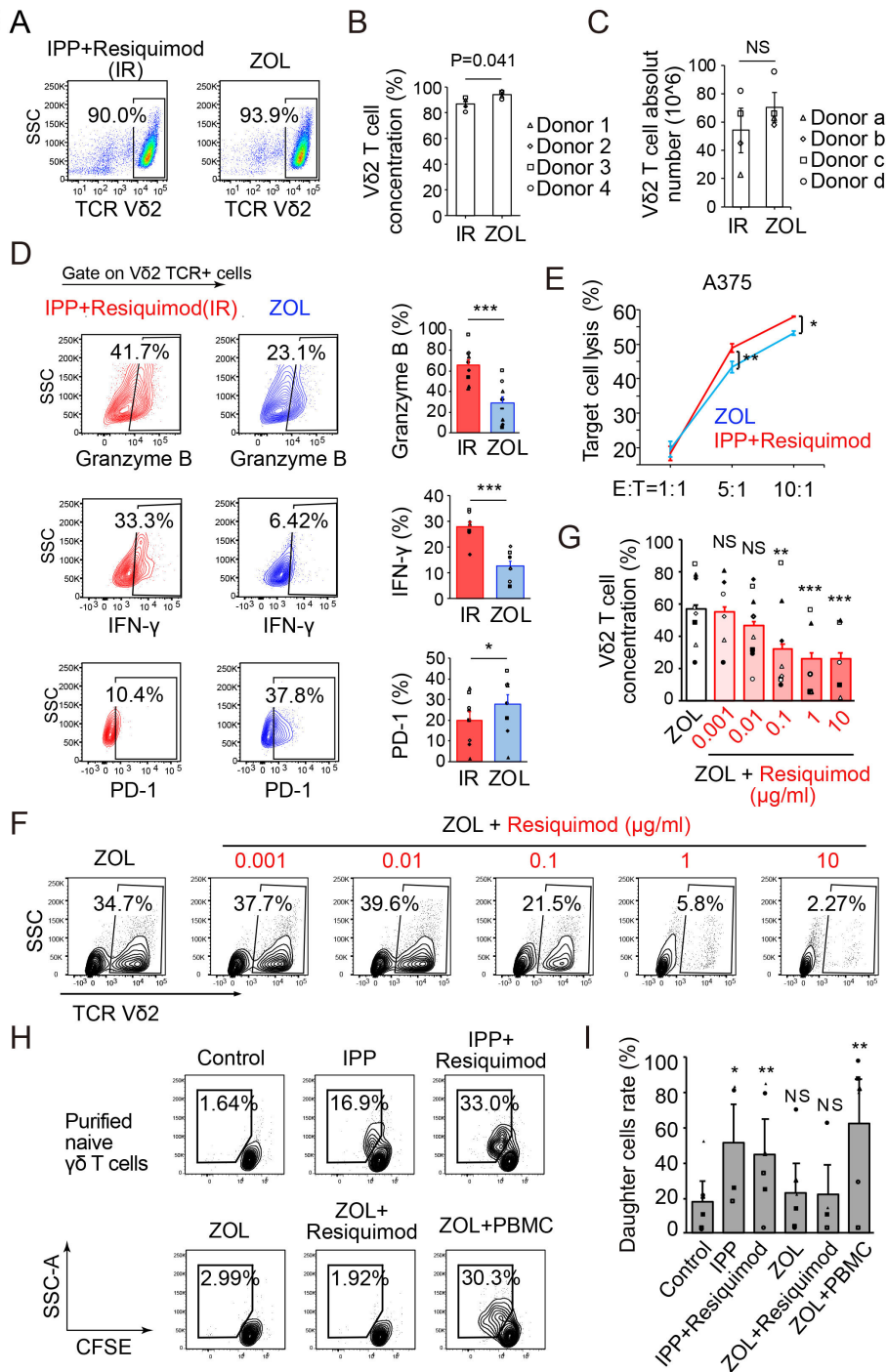


Figure 5 Advantage of Vδ2 T-cell expansion by IPP plus resiquimod over ZOL. (A–C) Vδ2 T-cell expansion using IPP plus resiquimod (IR) or ZOL. Two million PBMCs were added in each well with indicated stimulation for 10 days. Representative flowcharts (A) and statistical analysis results showing Vδ2 T-cell concentration (B) and absolute number (C, independent experiments) of Vδ2 T cells expanded by IPP plus resiquimod or ZOL from PBMCs on day 10, n=4. Data are shown as mean±SEM. P value is labeled. (D) Functional marker expression on Vδ2 T cells expanded by IPP plus resiquimod or ZOL from PBMCs on day 8 and statistical analysis. Data are shown as mean±SEM, n≥7. (E) LDH assay results showing the cytotoxicity of Vδ2 T cells expanded and sorted by IPP plus resiquimod or ZOL from PBMCs to melanoma cells A375 in vitro using different E:T ratios, n=3. Data are presented as mean±SEM. (F,G) Representative flowcharts (F) and statistical analysis (G) results showing resiquimod do not promote ZOL stimulation of Vδ2 T-cell proliferation from PBMCs in low concentration and inhibits its function in higher concentrations. Data are presented as mean±SEM. (H,I) CFSE proliferation assay of purified naive γδ T cells. Purified naive γδ T cells were labeled with CFSE and stimulated with IPP plus resiquimod or ZOL for 3 days. PBMCs from the same donor were not labeled with CFSE and used in the ZOL +PBMC group. Representative flowcharts are shown in (H) and statistical analysis in (I). Data are presented as mean±SEM. *P<0.05, **P<0.01, ***P<0.001. E:T, effector:target; IFN-γ, interferon gamma; IPP, isopentnyl pyrophosphate; LDH, lactate dehydrogenase; NS, no significant difference; PBMC, peripheral blood mononuclear cell; TCR, T-cell receptor; ZOL, zoledronic acid.

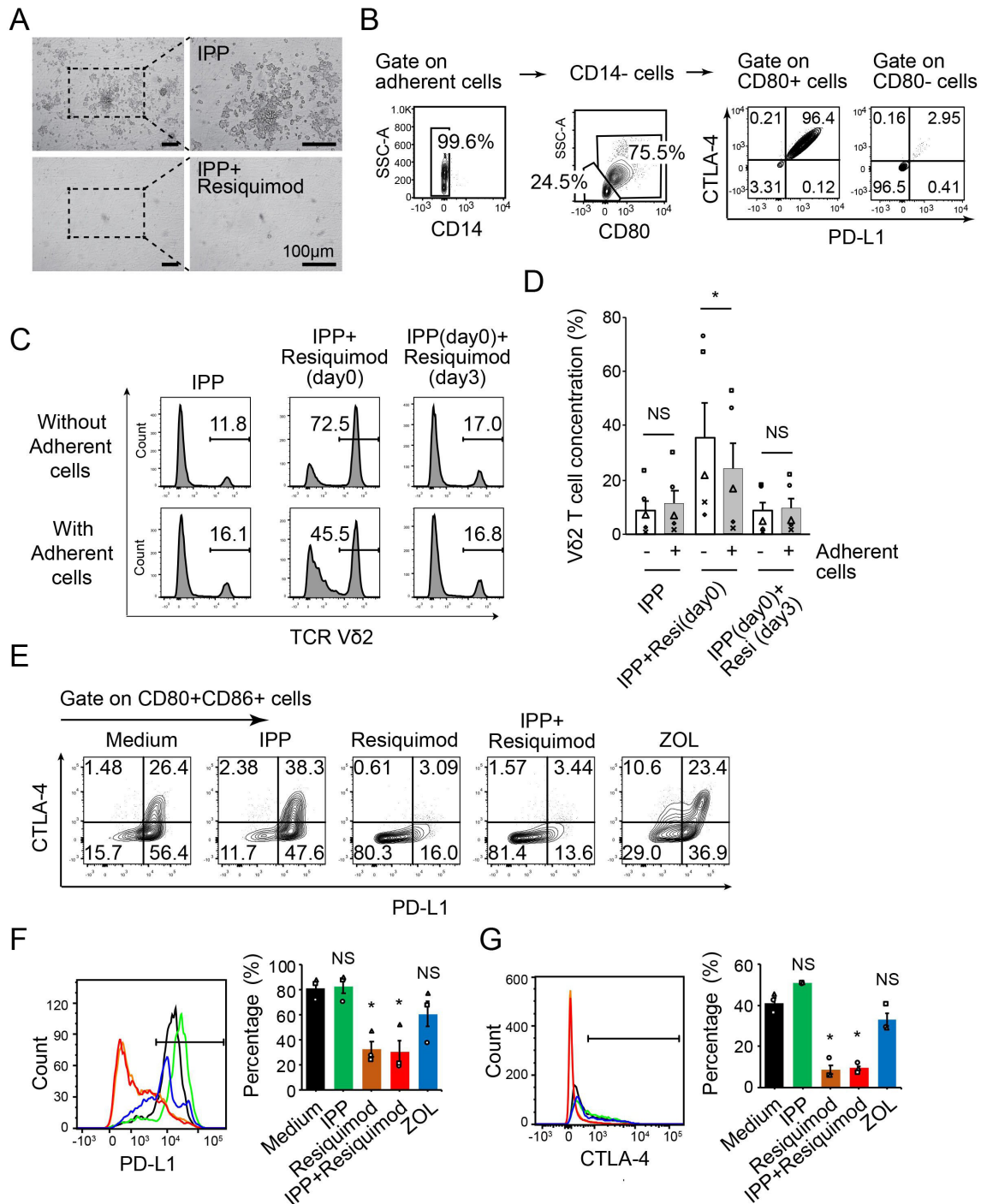


Figure 6 TLR7/8 activation suppresses formation and inhibitory function of adherent APCs. (A) Adherent cells during V δ 2 T expansion from PBMCs. Representative bright-field images (phase-contrast) of adherent cells from PBMCs cultured with IPP or IPP plus resiquimod on day 3. Scale bar, 100 μ m. (B) Adherent CD14⁻CD80⁺APC cells induced by IPP express both PD-L1 and CTLA-4. Representative flowcharts to characterize adherent cells after culturing PBMCs with IPP for 3 days. The adherent cells are mostly CD14⁻. A majority of these adherent cells are CD14⁻CD80⁺APCs. (C,D) Inhibitory function of adherent APCs. Adherent APCs were induced by culturing PBMCs for 3 days. The adherent APCs were collected and then added to PBMCs that have been stimulated with IPP and IPP plus resiquimod for 3 days; concentrations of V δ 2 T cells were measured by FACS 3 days later. In a separate group (IPP day 0+resiquimod day 3), both adherent cells and resiquimod were added to PBMCs that have been stimulated with IPP for 3 days. Representative flowcharts are shown in (C) and statistical analysis in (D). Data are shown as mean \pm SEM, n=5. (E–G) Flow cytometry and statistical analysis showing PD-L1 and CTLA-4 expression on CD80⁺CD86⁺ cells in cultured PBMCs with indicated stimulations. Representative flowcharts of PD-L1 and CTLA-4 expression (E), merged PD-L1 and CTLA-4 expression from a single donor and aggregated PD-L1 and CTLA-4 data from different donors are shown in (F,G), respectively. n=3, Data are shown as mean \pm SEM. *P<0.05, APC, antigen-presenting cell; IPP, isopentnyl pyrophosphate; NS, no statistical significance; PBMC, peripheral blood mononuclear cell; TCR, T-cell receptor; ZOL, zoledronic acid.

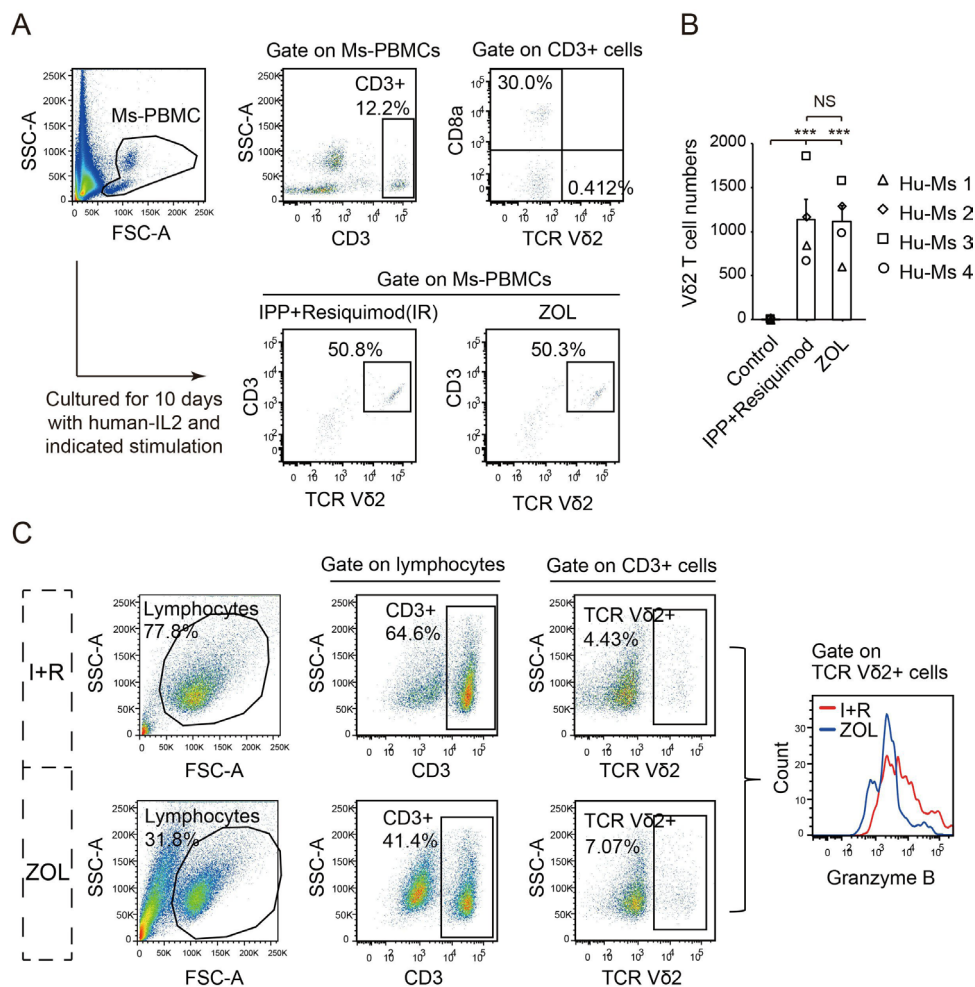


Figure 7 Human $\gamma\delta$ T cells in Hu-mice. (A) Human V δ 2 T cells in Hu-mice blood. Hu-mice blood was collected and analyzed by FACS or cultured with IPP plus resiquimod or ZOL. Flow cytometry results showing human T-cell population (using antihuman-CD3 antibodies) and few V δ 2 T cells in Hu-mice blood. V δ 2 T cells increased significantly after expansion for 10 days. (B) Absolute number of V δ 2 T cells expanded by IPP plus resiquimod or ZOL, results shown as mean \pm SEM, n=4. (C) Human V δ 2 T cells in Hu-mice spleen. Flow cytometry results show the percentage of human V δ 2 T cells in the spleen. Portion of mouse spleen was digested and cultured with IPP plus resiquimod or ZOL. Functional marker expression levels of Hu-mice spleen V δ 2 T lymphocytes. ***P<0.001. Hu-mice, humanized mice; IL, interleukin; IPP, isopentnyl pyrophosphate; I+R, IPP plus resiquimod; NS, no significance; PBMC, peripheral blood mononuclear cell; TCR, T-cell receptor; ZOL, zoledronic acid.

V δ 2 T-cell expansion in Hu-mice

NSG mice that were engrafted with human hematopoietic stem (CD34+) cells or peripheral blood leukocytes (Hu-mice) are a useful tool to study immunotherapy¹⁹; however, it is unclear whether these mice have functional human $\gamma\delta$ T cells. Here, we showed that CD3+V δ 2+ T cells were in the PBMCs of Hu-mice (figure 7A). We cultured PBMCs from four Hu-mice using human PBMCs culture media and stimulated them with IPP plus resiquimod or ZOL for 10 days. Peripheral V δ 2 T cells in Hu-mice responded to the stimulations and showed approximately a thousand times of expansion (figure 7B). V δ 2 T from Hu-mice expanded by IPP plus resiquimod showed more granzyme B expression than by ZOL (figure 7C). These data show that Hu-mice engrafted human peripheral V δ 2 T cells and may be a useful preclinical model for $\gamma\delta$ T-cell functional study.

DISCUSSION

$\gamma\delta$ T cells are a good candidate for ACT,¹⁰ but their potential has not been fully realized in the clinic. To better use $\gamma\delta$ T cells for therapy, we discovered a costimulation strategy that activates $\gamma\delta$ TCR and TLR7/8 using a natural and less potent pAg, IPP, and a potent TLR7/8 agonist, resiquimod to expand V δ 2 T cells from PBMCs. The combination of IPP and resiquimod induces efficient V δ 2 T-cell expansion and produces V δ 2 T cells with better antitumor function and lower PD-1 expression than V δ 2 T cells expanded by ZOL.

Several established methods have been used to obtain a sufficient number of V δ 2 T cells from PBMCs for therapy.¹³ Most of the clinical studies used ZOL to expand V δ 2 T cells from PBMCs.¹⁴ The efficacy of adoptive cell transfer of V δ 2 T cells is suboptimal despite minimal adverse events being observed.^{11 14} The failures of such

a strategy is most likely related to insufficient $\gamma\delta$ TCR responses,¹¹ activation-induced cell death, functional exhaustion, and aging of T cells before encountering target cells.³¹ Recently, Kouakanou *et al* reported that vitamin C promoted the expansion and function of $\gamma\delta$ T cells; however, the method was only effective for purified naïve cells.³² Inspired by the manner of costimulation in $\alpha\beta$ T cells,³³ we found that V δ 2 T cells respond to costimulation from $\gamma\delta$ TCR and TLR7/8 activation. Our method can be used to expand both purified V δ 2 T cells and V δ 2 T cells in PBMCs.

Unlike $\alpha\beta$ T cells, the full activation of $\gamma\delta$ T cells does not require both signal one and signal two from $\gamma\delta$ TCR and costimulatory pathways. However, stimulation through $\gamma\delta$ TCR and costimulatory pathways (such as CD27, CD28, and 4-1BB), cytokine receptors,³¹ NKG2D, and TLRs^{7,34} can enhance the response and function of $\gamma\delta$ T cells. Serrano *et al* recently demonstrated that TLR8 ligands (resiquimod, TL8-506 and motolimod) potently stimulated the pAg-induced IFN- γ production in the V δ 2 T cells. However, these compounds suppressed the in vitro expansion of V δ 2 T cells in response to ZOL or HMBPP.²⁸ A similar finding was observed in our study when we combined resiquimod with ZOL during V δ 2 T-cell expansion. HMBPP is known to be 10,000 times more potent than IPP³⁵ and ZOL is also a potent bisphosphonate. Our study surprisingly showed that resiquimod does not inhibit IPP-induced V δ 2 T-cell expansion but significantly enhances V δ 2 cell expansion. The resulting V δ 2 T cells expressed lower levels of PD-1 and had better antitumor activity than V δ 2 T cells expanded by ZOL. These results suggest that optimizing $\gamma\delta$ TCR stimulation intensity is crucial for designing costimulation strategies for V δ 2 T-cell expansion.

A scRNA-seq study of purified $\gamma\delta$ T cells performed by Jean Jacques Fournié and colleagues offered a landmark transcriptomic resource for analyzing the gene expression of $\gamma\delta$ T cells during activation and maturation.²² Reanalysis of that dataset showed the PI3K–Akt–mTOR pathway played a crucial role in the activation, proliferation, and maturation of V δ 2 T cells. Our RPPA data demonstrated that coactivation of $\gamma\delta$ TCR with IPP and resiquimod enhanced the phosphorylation levels of the PI3K–Akt–mTOR pathway in V δ 2 T cells. Inhibition of this pathway using rapamycin or Torin abolished this effect. Similarly, inhibition of TLR7/8–MyD88 pathway also suppressed V δ 2 proliferation. MyD88 is known to affect the function of PI3K–Akt–mTOR pathway in T cells. These data support that TLR7/8 activation acts as a costimulatory signal to enhance V δ 2 T-cell expansion.

APCs play an important role in bisphosphates (such as ZOL) and pAgs induced expansion of V δ 2 T cells by releasing soluble IPP. The majority of APC cells during PBMCs culturing are CD14+ monocyte-derived dendritic cells (Mo-DCs) which are characterized by their adherence.^{36,37} pAgs recognition of V δ 2T cells relies matured Mo-DCs.³⁴ Our data confirmed that

APCs are indispensable during ZOL-mediated V δ 2 T-cell expansion. Recently, Serrano *et al* found that the TLR8 and TLR7/8 ligands promote V δ 2 T-cell functions via a monocytes-dependent costimulation manner³⁸ and also showed a critical role of monocyte-derived cytokines such as IL-1 β , IL-18 and others.^{38,39} Immature DCs can inhibit functional T cells in vitro.⁴⁰ We analyzed the phenotypes of adherent Mo-DCs and identified them as APCs playing inhibitory function with high-level expression of PD-L1 and CTLA-4.³⁰ TLR agonists are known to promote APC maturation and function.⁴¹ We discovered that resiquimod significantly decreased the number of adherent Mo-DCs and the expression of PD-L1 and CTLA-4 in the CD80+ CD86+APCs. For the first time, we demonstrate that activation of TLR7/8 inhibits the expression of checkpoint proteins on the APCs, which contributes to better IPP-induced V δ 2 T-cell expansion and function.

Costimulation of IPP and resiquimod promoted V δ 2 T-cell cytotoxicity to tumor cells both in vitro and in vivo. Nevertheless, we noticed that $\gamma\delta$ T cells cannot survive long in nude mouse xenograft model, and it is not possible to study tumor homing and infiltration using this model. Humans have evolved specific $\gamma\delta$ T-cell subsets that are different from rodents, which severely limit the study of human $\gamma\delta$ development and function in mouse models. To overcome this limitation, we evaluated the potential of Hu-mice as a model for $\gamma\delta$ T-cell studies. We found that $\gamma\delta$ T cells could be identified in multiple organs with the highest concentration in the spleen. Peripheral V δ 2 T cells from Hu-mice PBMCs and spleen could be significantly expanded by IPP plus resiquimod or ZOL. Expanded V δ 2 T cells had similar surface marker expression as V δ 2 T cells from human PBMCs. Nevertheless, generating Hu-mice is time consuming and costly. The model needs to be further refined to study V δ 2 T-cell homing and its impact on the tumor microenvironment.

In conclusion, our studies demonstrate that IPP plus resiquimod enhances proliferation and antitumor activity of V δ 2 T cells. Resiquimod promotes the expansion of V δ 2 T cells through activating the TLR7/8–MyD88 and mTOR signaling pathways and regulates the differentiation and inhibitory function of APCs. The data support that the combination of IPP with resiquimod may be used to expand V δ 2 T cell ex vivo for adoptive cell immunotherapy.

Author affiliations

¹Department of Pathology and Laboratory Medicine, The University of Pennsylvania, Philadelphia, Pennsylvania, USA

²National Key Laboratory for Novel Software Technology, Nanjing University, Nanjing, China

³State Key Laboratory of Membrane Biology, Institute of Zoology, Chinese Academy of Science, Beijing, China

⁴Molecular and Cellular Oncogenesis Program, The Wistar Institute, Philadelphia, Pennsylvania, USA

⁵Department of Neurosurgery, School of Medicine, Duke University, Durham, North Carolina, USA

⁶Center for Cellular Immunotherapies, Perlman School of Medicine, The University of Pennsylvania, Philadelphia, Pennsylvania, USA

⁷Division of Hematology/Oncology, Department of Medicine, Perelman School of Medicine, The University of Pennsylvania, Philadelphia, Pennsylvania, USA

⁸Department of Radiation Oncology, The University of Pennsylvania, Philadelphia, Pennsylvania, USA

⁹Parker Institute for Cancer Immunotherapy, The University of Pennsylvania, Philadelphia, Pennsylvania, USA

¹⁰Cell, Developmental and Cancer Biology, School of Medicine, Oregon Health and Science University, Portland, Oregon, USA

¹¹Department of Biology, The University of Pennsylvania, Philadelphia, Pennsylvania, USA

Acknowledgements We thank Dr Jean Jacques Fournié, University of Toulouse, France, for sharing unpublished data.

Contributors XX, HW, and HC designed the subject; XX, HW, MH, RS, GM, WG, CHJ, JS, AH, TM, and YF discussed the subject and experiments; HW, HC, ST, LO, and LD performed flow cytometry and analysis; HW, HC, LO, YG, and LH performed ex vitro cytotoxicity assays; HL, JZ, and HW performed single-cell RNA sequencing dataset analysis; GZ, HC, SL, and HW prepared the samples for reverse-phase protein array and analyzed the results; SL, HC, and HW performed the nude mouse xenograft experiments; MH, RS, RC, TC, and LL developed humanized mice; representative figures were selected for publication by XX, HW, and HC; XX, HW, AH, and RS wrote the manuscript; and every author reviewed the manuscript. XX is responsible for the overall content.

Funding The research was funded by the National Institutes of Health (grant numbers CA114046 and CA174523) and Tara Miller Melanoma Foundation.

Competing interests XX, HW, HC and LO are listed as inventors on a patent owned by the University of Pennsylvania related to this work. XX and WG are scientific founders of CureBioTech and Exio Biosciences. CHJ is a scientific founder of Tmunity Therapeutics.

Patient consent for publication Not applicable.

Ethics approval This study was approved by the Institution Review Board at the University of Pennsylvania.

Provenance and peer review Not commissioned; externally peer reviewed.

Data availability statement Data are available in a public, open access repository. All data relevant to the study are included in the article or uploaded as supplementary information. Reverse-phase protein array data are available as supplementary information. Single-cell sequence data could be obtained from NCBI GEO data set repository GSE128223 and described in the Methods section.

Supplemental material This content has been supplied by the author(s). It has not been vetted by BMJ Publishing Group Limited (BMJ) and may not have been peer-reviewed. Any opinions or recommendations discussed are solely those of the author(s) and are not endorsed by BMJ. BMJ disclaims all liability and responsibility arising from any reliance placed on the content. Where the content includes any translated material, BMJ does not warrant the accuracy and reliability of the translations (including but not limited to local regulations, clinical guidelines, terminology, drug names and drug dosages), and is not responsible for any error and/or omissions arising from translation and adaptation or otherwise.

Open access This is an open access article distributed in accordance with the Creative Commons Attribution Non Commercial (CC BY-NC 4.0) license, which permits others to distribute, remix, adapt, build upon this work non-commercially, and license their derivative works on different terms, provided the original work is properly cited, appropriate credit is given, any changes made indicated, and the use is non-commercial. See <http://creativecommons.org/licenses/by-nc/4.0/>.

ORCID iDs

Huaishan Wang <http://orcid.org/0000-0002-8686-4357>

Xiaowei Xu <http://orcid.org/0000-0003-4098-7690>

REFERENCES

- June CH, O'Connor RS, Kawalekar OU, *et al.* CAR T cell immunotherapy for human cancer. *Science* 2018;359:1361–5.
- Rosenberg SA, Restifo NP. Adoptive cell transfer as personalized immunotherapy for human cancer. *Science* 2015;348:62–8.
- Kalos M, June CH. Adoptive T cell transfer for cancer immunotherapy in the era of synthetic biology. *Immunity* 2013;39:49–60.
- Khong HT, Restifo NP. Natural selection of tumor variants in the generation of "tumor escape" phenotypes. *Nat Immunol* 2002;3:999–1005.
- Kabelitz D, Serrano R, Koukanou L, *et al.* Cancer immunotherapy with $\gamma\delta$ T cells: many paths ahead of US. *Cell Mol Immunol* 2020;17:925–39.
- Godder KT, Henslee-Downey PJ, Mehta J, *et al.* Long term disease-free survival in acute leukemia patients recovering with increased gammadelta T cells after partially mismatched related donor bone marrow transplantation. *Bone Marrow Transplant* 2007;39:751–7.
- Wesch D, Peters C, Oberg H-H, *et al.* Modulation of $\gamma\delta$ T cell responses by TLR ligands. *Cell Mol Life Sci* 2011;68:2357–70.
- Dar AA, Patil RS, Chiplunkar SV. Insights into the relationship between toll like receptors and gamma delta T cell responses. *Front Immunol* 2014;5:366.
- Pietschmann K, Beetz S, Welte S, *et al.* Toll-like receptor expression and function in subsets of human gammadelta T lymphocytes. *Scand J Immunol* 2009;70:245–55.
- Vantourout P, Hayday A. Six-of-the-best: unique contributions of $\gamma\delta$ T cells to immunology. *Nat Rev Immunol* 2013;13:88–100.
- Hoeres T, Smetak M, Pretscher D, *et al.* Improving the efficiency of V γ 9V δ 2 T-cell immunotherapy in cancer. *Front Immunol* 2018;9:800.
- Eberl M, Hintz M, Reichenberg A, *et al.* Microbial isoprenoid biosynthesis and human gammadelta T cell activation. *FEBS Lett* 2003;544:4–10.
- Tan WK, Tay JC, Zeng J. Expansion of gamma delta T Cells-A short review on bisphosphonate and K562-Based methods. *J Immunol Sci* 2018;2.
- Sebestyen Z, Prinz I, Déchanet-Merville J, *et al.* Translating gammadelta ($\gamma\delta$) T cells and their receptors into cancer cell therapies. *Nat Rev Drug Discov* 2020;19:169–84.
- Watanabe D, Koyanagi-Aoi M, Taniguchi-Ikeda M, *et al.* The generation of human $\gamma\delta$ T cell-derived induced pluripotent stem cells from whole peripheral blood mononuclear cell culture. *Stem Cells Transl Med* 2018;7:34–44.
- Lim WA, June CH. The principles of engineering immune cells to treat cancer. *Cell* 2017;168:724–40.
- Liu S, Zhang G, Guo J, *et al.* Loss of Phd2 cooperates with BRAF^{V600E} to drive melanomagenesis. *Nat Commun* 2018;9:5426.
- Lu H, Liu S, Zhang G, *et al.* PAK signalling drives acquired drug resistance to MAPK inhibitors in BRAF-mutant melanomas. *Nature* 2017;550:133–6.
- Somasundaram R, Connelly T, Choi R, *et al.* Tumor-infiltrating mast cells are associated with resistance to anti-PD-1 therapy. *Nat Commun* 2021;12:346.
- Zhu Y, Wang H, Xu Y, *et al.* Human $\gamma\delta$ T cells augment antigen presentation in *Listeria Monocytogenes* infection. *Mol Med* 2016;22:737–46.
- Ou L, Wang H, Liu Q, *et al.* Dichotomous and stable gamma delta T-cell number and function in healthy individuals. *J Immunother Cancer* 2021;9:e002274.
- Pizzolato G, Kaminski H, Tosolini M, *et al.* Single-cell RNA sequencing unveils the shared and the distinct cytotoxic hallmarks of human TCRV δ 1 and TCRV δ 2 $\gamma\delta$ T lymphocytes. *Proc Natl Acad Sci U S A* 2019;116:11906–15.
- Stuart T, Butler A, Hoffman P, *et al.* Comprehensive integration of single-cell data. *Cell* 2019;177:e1821:1888–902.
- Huang DW, Sherman BT, Lempicki RA. Systematic and integrative analysis of large gene lists using DAVID bioinformatics resources. *Nat Protoc* 2009;4:44–57.
- Wang H, Zhai K, Xue Y, *et al.* Global deletion of TSPO does not affect the viability and gene expression profile. *PLoS One* 2016;11:e0167307.
- Hänzelmann S, Castelo R, Guinney J. GSVA: gene set variation analysis for microarray and RNA-seq data. *BMC Bioinformatics* 2013;14:1–15.
- Cancer Genome Atlas Network. Comprehensive molecular portraits of human breast tumours. *Nature* 2012;490:61–70.
- Serrano R, Wesch D, Kabelitz D. Activation of human $\gamma\delta$ T cells: modulation by toll-like receptor 8 ligands and role of monocytes. *Cells* 2020;9:713.
- Kabelitz D, Serrano R, Koukanou L, *et al.* Cancer immunotherapy with $\gamma\delta$ T cells: many paths ahead of US. *Cell Mol Immunol* 2020;17:925–39.
- Wang XB, Fan ZZ, Anton D, *et al.* CTLA4 is expressed on mature dendritic cells derived from human monocytes and influences their maturation and antigen presentation. *BMC Immunol* 2011;12:21.
- Ribeiro ST, Ribot JC, Silva-Santos B. Five layers of receptor signaling in $\gamma\delta$ T-cell differentiation and activation. *Front Immunol* 2015;6:15.

- 32 Kouakanou L, Xu Y, Peters C, *et al.* Vitamin C promotes the proliferation and effector functions of human $\gamma\delta$ T cells. *Cell Mol Immunol* 2020;17:462–73.
- 33 Garlie NK, LeFever AV, Siebenlist RE, *et al.* T cells coactivated with immobilized anti-CD3 and anti-CD28 as potential immunotherapy for cancer. *J Immunother* 1999;22:336–45.
- 34 Devilder M-C, Allain S, Dousset C, *et al.* Early triggering of exclusive IFN-gamma responses of human Vgamma9Vdelta2 T cells by TLR-activated myeloid and plasmacytoid dendritic cells. *J Immunol* 2009;183:3625–33.
- 35 Xia M, Hesser DC, De P, *et al.* A subset of protective $\gamma\delta$ 2 T cells is activated by novel mycobacterial glycolipid components. *Infect Immun* 2016;84:2449–62.
- 36 Zhou LJ, Tedder TF. CD14+ blood monocytes can differentiate into functionally mature CD83+ dendritic cells. *Proc Natl Acad Sci U S A* 1996;93:2588–92.
- 37 Wang X, Borquez-Ojeda O, Stefanski J, *et al.* Depletion of high-content CD14+ cells from apheresis products is critical for successful transduction and expansion of CAR T cells during large-scale cGMP manufacturing. *Mol Ther Methods Clin Dev* 2021;22:377–87.
- 38 Serrano R, Coch C, Peters C, *et al.* Monocyte-dependent co-stimulation of cytokine induction in human $\gamma\delta$ T cells by TLR8 RNA ligands. *Sci Rep* 2021;11:1–13.
- 39 Takimoto R, Suzawa T, Yamada A, *et al.* Zoledronate promotes inflammatory cytokine expression in human CD14-positive monocytes among peripheral mononuclear cells in the presence of $\gamma\delta$ T cells. *Immunology* 2021;162:306–13.
- 40 Dhodapkar MV, Steinman RM, Krasovsky J, *et al.* Antigen-specific inhibition of effector T cell function in humans after injection of immature dendritic cells. *J Exp Med* 2001;193:233–8.
- 41 Dar AA, Patil RS, Chipunkar SV. Insights into the relationship between toll like receptors and gamma delta T cell responses. *Front Immunol* 2014;5:366.